Lithos 316–317 (2018) 66–76

Contents lists available at ScienceDirect

Lithos

journal homepage: www.elsevier.com/locate/lithos

From ocean to mantle: new evidence for U-cycling with implications for the HIMU source and the secular Pb isotope evolution of Earth's mantle

Thomas Pettke [a,*], János Kodolányi [a,b], Balz S. Kamber [c]

[a] University of Bern, Institute of Geological Sciences, Baltzerstrasse 1+3, CH-3012 Bern, Switzerland
[b] Max Planck Institute for Chemistry, Hahn-Meitner-Weg 1, 55128 Mainz, Germany
[c] Department of Geology, School of Natural Sciences, Trinity College Dublin, Dublin 2, Ireland

ARTICLE INFO

Article history:
Received 13 November 2017
Accepted 6 July 2018
Available online 9 July 2018

Keywords:
Ocean island basalt
Mantle metasomatism
Supercritical liquid
Subduction element processing
Lead isotope systematics

ABSTRACT

Of the isotopically distinctive mantle domains, the so-called HIMU ("high-μ"; $\mu = {}^{238}U/{}^{204}Pb$) source is the most extreme, and its genesis continues to be debated. We report very strong U enrichment at unchanged Th concentrations in Cretaceous oceanic serpentinites with exceptionally high $^{206}Pb/^{204}Pb$ (reaching 56) but unchanged $^{208}Pb/^{204}Pb$. Similar, but less extreme, features are found in 1.9 billion years old altered oceanic crust (AOC). Forward modelling demonstrates that mantle, if metasomatised by supercritical liquids derived from AOC and serpentinites, evolves to the HIMU Pb isotope signatures, while satisfying experimental and empirical constraints on subduction zone element processing. By contrast, no model solutions for the conventional proposal of the HIMU source representing residual igneous altered oceanic crust can be reconciled with $^{208}Pb/^{204}Pb$, strengthening the need for a paradigm shift regarding HIMU OIB genesis. Over time, the net U addition to the convecting mantle via deeply subducted serpentinite has expressed itself as the so-called second terrestrial Pb isotope paradox, or kappa conundrum.

1. Introduction

The inventory of U dissolved in seawater is orders of magnitude higher than that of Th and Pb (e.g., Chen et al., 1986). Shortly after their emplacement along mid-ocean ridges, oceanic basalts and mantle rocks become enriched in U over Th and Pb, owing to interaction with seawater (e.g., Niu, 2004; Staudigel et al., 1995). Over the last 2.35 billions of years (Ga), subduction recycling of altered oceanic crust (AOC) is thus thought to have modified the Pb-isotope composition of the convecting mantle as a whole (Elliott et al., 1999; Kramers and Tolstikhin, 1997; Kumari et al., 2016) and the mantle source regions of certain ocean island basalt (OIB) groups in particular (Chase, 1981; Chauvel et al., 1992; Staudigel et al., 1995; Stracke, 2012; Weaver, 1991; Zindler and Hart, 1986). In spite of the wide acceptance of this idea, there is a surprising paucity of direct supporting observations from the geochemistry of altered ocean floor materials, and details of the recycling process continue to be debated (Andersen et al., 2015; Bach et al., 2001; Cabral et al., 2013; Castillo, 2015; Chauvel et al., 1992; Halliday et al., 1992; Hanyu et al., 2014; Hart and Staudigel, 1989; Jackson et al., 2015; Kamber and Collerson, 1999; Kelley et al., 2005; Li et al., 2014; Nebel et al., 2013; Pilet et al., 2008; Ryan and Chauvel, 2014; Staudigel, 2014; Stracke, 2012; Weiss et al., 2016; White, 2015).

Hydrated peridotite (serpentinite) and oceanic crust are the main carriers of water into deep subduction zones, causing strong relative re-enrichments of the mantle in specific elements, including U. Ocean floor serpentinites are arguably the best recorders of seawater-derived fluid alteration of igneous oceanic lithosphere. This is because previous melt extraction leaves these rocks (originally representing depleted MORB source mantle; DMM) severely depleted in all incompatible elements, including U, Th, and Pb. Any later incompatible element addition from seawater during serpentinisation is therefore readily quantified (Kodolányi et al., 2012; Niu, 2004; Paulick et al., 2006).

This study presents new Pb isotope data and U, Th, and Pb concentrations for carefully selected and previously characterised (Kodolányi et al., 2012) oceanic serpentinites from ODP Leg 210 (Supplementary Fig. 1), which represent the hydrated part of the mantle section of modern (~120 Ma; Robertson, 2007) ocean floor. The paper also discusses data from the 1.89 Ga old seafloor-altered high-Mg basalts of the Flin Flon assemblage (Trans-Hudson orogen, Canada), a prominent Paleoproterozoic AOC characterised in detail previously (Babechuk and Kamber, 2011; Stern et al., 1995), as a possible source for HIMU OIB. This empirical dataset from an ancient AOC is compared to modern AOC Composites representing compiled data from oceanic sections (Bach et al., 2003; Kelley et al., 2003), and these data were used to explore, by modelling, whether seawater-derived U could have contributed to produce the source of HIMU (high-μ, where $\mu = {}^{238}U/{}^{204}Pb$) OIBs. This important type of OIB, with a high time-integrated

* Corresponding author.
E-mail address: pettke@geo.unibe.ch (T. Pettke).

https://doi.org/10.1016/j.lithos.2018.07.010

$^{238}U/^{204}Pb$, and present-day $^{206}Pb/^{204}Pb$ (>20.5), low $^{87}Sr/^{86}Sr$ (<0.703), and $^{143}Nd/^{144}Nd$ ratios between 0.5128 and 0.5130, is compositionally the least heterogeneous of all isotopic families of OIBs, and it is one of the four principal source components required to account for >99% of all known OIB Sr, Nd, and Pb isotope signatures (Stracke, 2012).

2. Methods

2.1. Serpentinite Pb isotope and U-Th-Pb concentration measurements

Serpentinite samples for bulk rock trace element and Pb isotope ratio analyses were selected from a larger collection previously characterised geochemically in great detail (Kodolányi et al., 2012). For all samples, a 100 mg aliquot was initially bomb-digested (steel-jacketed Teflon vessel, HF-HNO_3, 190 °C, 72 h). A small (ca. 2.6%) liquid aliquot of this digest was used for the trace element analysis; the remainder was kept for Pb isotope analysis. Trace element measurements were performed with an X Series II (Thermo Fisher Scientific) quadrupole ICP-MS system at Laurentian University (Sudbury, Canada). Lead isotope ratios were also measured on this instrument, operated in a clean-room HEPA-filtered environment and with a Hg-poor Ar supply, after purification using miniaturised HBr-HCl chemistry. Analytical details are reported in Supplementary Information 1.

2.2. Details of the Pb isotope forward model

It is widely discussed that AOC may be an important source of U, Th, and Pb for the peculiar HIMU OIB endmember. To approximate AOC we used data from the 1.89 Ga old seafloor-altered high-Mg basalts of the Flin Flon assemblage (Trans-Hudson orogen, Canada), the most pristine Paleoproterozoic AOC known to date, as well as AOC Composites from the literature. Calculation of forward models to predict the Pb isotope evolution of contrasting subduction zone source components requires the following parameters:

(1) The first is the initial Pb isotope composition of ancient AOC. The values used here are: $^{206}Pb/^{204}Pb = 15.480 \pm 75$; $^{207}Pb/^{204}Pb = 15.165 \pm 24$; $^{208}Pb/^{204}Pb = 35.042 \pm 44$. They represent the average initial isotope ratios of 8 least radiogenic samples of the Moen Bay suite (ELB010-012, ELB015-019, and ELB023; Babechuk and Kamber, 2011), which are the most N-MORB-like rocks of the Paleoproterozoic Flin Flon ocean floor basalt series. The selected 8 samples show transition metal evidence for VMS (volcanogenic massive sulphide) alteration and are characterised by depleted but uniform high field strength element (HFSE) concentrations along with prominent Pb and relative U enrichments, resulting in very low μ and the lowest measured Th/U ($^{232}Th/^{238}U = \kappa \approx 1.8$) of this series (Fig. 7b of Babechuk and Kamber, 2011). It should be noted that the initial isotope ratios chosen here are more radiogenic than those of single stage mantle evolution curves. This is because of the unrealistically low μ of the single-stage models, which have since been replaced with multi-stage (e.g., Stacey and Kramers, 1975) or dynamic μ (e.g., Kramers and Tolstikhin, 1997) terrestrial differentiation models. The preferred initial Pb-isotope composition is also higher in $^{207}Pb/^{204}Pb$ than the contemporaneous depleted mantle composition of Kramers and Tolstikhin (1997). This is a common feature as very similar compositions are recorded by least radiogenic ores from the coeval Cape Smith belt further east in the Trans-Hudson orogeny and ores from the similarly aged Ashanti gold fields hosted in juvenile greenstones in West Africa (see Fig. 13 of Babechuk and Kamber, 2011). Regardless, the 1.9 Ga initial isotope composition can be considered as being well constrained.

(2) The second parameter are the original U-Th-Pb ratios of the AOC, i.e., those prevailing prior to subduction processing. They were calculated as the average μ (10.75) and κ (2.31) of all the 47 Flin Flon metabasalts (omitting 1 out 48 samples, APL008, which is a cross-cutting, incompatible element-enriched dyke). These rocks have experienced greenschist facies metamorphism but detailed geochemical analysis has shown that Th/U systematics were only affected by rare contact metamorphism (Babechuk and Kamber, 2011), samples of which were avoided for this study.

(3) The age of the HIMU OIB source was taken as 1.9 Ga to calculate the time-integrated $^{206}Pb/^{204}Pb$, $^{207}Pb/^{204}Pb$, and $^{208}Pb/^{204}Pb$ ratios in 0.1 Ga steps. The 1.9 Ga age is similar to the average time originally postulated by Chase (1981) for ageing of the HIMU OIB source component;

(4) The fourth set of parameters concerns U/Th/Pb fractionation in the subducted AOC that was assessed in a two-stage process. The subducted AOC is modified via aqueous fluid loss at stage A at subarc depth (5% fluid loss at 4 GPa/800 °C). This is then followed by stage B subduction dehydration that generates the source component characteristic of HIMU lavas from the residue of stage A. It is a 2% supercritical liquid loss at ca. 6 GPa/~1100 °C, which affects the chemistry of the dehydrated slab residue and defines the metasomatising fluid agent. Subduction fractionation of U/Th/Pb is based on the experimental data set for the K-free basalt-water system at the relevant pressures (Kessel et al., 2005a). This work was the first to quantify, by direct measurement, element concentrations and thus element abundance ratios in aqueous fluids as well as supercritical liquids in equilibrium with basaltic eclogite residue at subarc depths and beyond. Other data sets published to date investigated different compositional systems or quantified element distribution upon partial melting of basaltic compositions.
Stage A: The μ of the residual Flin Flon AOC increases after this shallow fluid escape by a factor of 2 to 21.5, because Pb is removed much more efficiently than U upon subduction devolatilisation (compare Fig. 2a). The factor of 2 is the result of ~50% loss of Pb upon 5% shallow fluid escape along with very modest U loss. Because Th has even lower $D_{(fluid/solid)}$ than U at these conditions (Kessel et al., 2005a), κ was assumed to remain unmodified in the residue.
Stage B: At this stage, a supercritical liquid is generated. Because Pb and U are about equally mobile at these conditions, the μ of 2% supercritical liquid derived from AOC remains unmodified at 21.5. Accordingly, the μ of the dehydrated slab residue also remains unmodified at 21.5. By contrast, mobilities for U and Th significantly differ at these conditions. Due to the greater mobility of Th over U in supercritical liquids (prominently so for T ≦ 1000 °C; compare Fig. 2b), the κ of the metasomatising supercritical liquid was increased by a factor of 1.3, to become 3.00. Accordingly, the κ of the residual AOC was lowered by a factor of 0.70 to become 1.62 (Fig. 2c). Note that Kessel et al. (2005a) did not list data for 1100 °C at 6 GPa; hence, the factors employed here were interpolated between those available for 1000 °C/6 GPa and for 1200 °C/6 GPa.

(5) For the metasomatised mantle peridotite endmember, it was assumed that the U, Th, and Pb added from slab devolatilisation completely overwhelmed the indigenous depleted mantle inventory of these elements. The initial Pb-isotope ratios for this source were therefore assumed to be identical to the estimate for the AOC (i.e.; $^{206}Pb/^{204}Pb = 15.480 \pm 75$; $^{207}Pb/^{204}Pb = 15.165 \pm 24$; $^{208}Pb/^{204}Pb = 35.042 \pm 44$); μ and κ values were selected as explained above.

(6) The same models were also run employing trace element inventories of modern AOC composites rather than the specific Paleoproterozoic Flin Flon metabasalts, because it might be argued that the latter could contain a small subduction zone component. Of the published modern AOC composites (e.g., Staudigel, 2014), old AOC is represented by ODP Site 801 (170 Ma crust;

Kelley et al., 2003), and young AOC by DSDP/ODP Hole 504B (~6.6 Ma crust; Bach et al., 2003), but we note that their chemistries vary prominently.

(7) Finally, net addition of U via aqueous fluid from the hydrous subducted mantle rocks to supercritical liquid expelled from AOC was also explored. Parameter definitions and model results for these additional models are provided in Supplementary information 2.

2.3. Details of AOC subduction trace element processing

Changes in primitive mantle (PM) normalised trace element abundance patterns with progressive subduction (i.e., the effects of subduction processing) were explored using the AOC Super Composite data of DSDP/ODP Hole 504B (Bach et al., 2003) and the measured fluid/residue element distribution coefficients for the K-free basalt-water system (Kessel et al., 2005a). We used AOC composite data in this case rather than a specific data set because such composites are intended to average out variability in element abundances arising from combined variations in extent of seafloor alteration and degree of mantle melting (Staudigel, 2014).

Henry's law trace element distribution mass balance calculations simulate the compositional evolution with progressive subduction. Aqueous fluid release at subarc depths of ca. 120 km (4 GPa / 800 °C; P-T estimates taken from subduction zone thermal models of Syracuse et al., 2010) was assumed to be 5 wt% (compare Schmidt and Poli, 2014). Lower aqueous fluid fractions produce the same residual eclogite pattern, however, with more limited offset from original AOC composite composition (inset of Fig. 4). The residual eclogite, which is water-free at the K-free composition used here, shows notable depletions in LILE and Pb, while the HFSE and middle to heavy REE remain essentially unchanged. There is no significant difference in composition of residual eclogite between one-step dehydration and incremental dehydration so long as the mass of fluid loss remains constant and is accomplished at roughly the same P and T, i.e., with comparable mineral-fluid assemblages. Stabilising certain accessory minerals in the residue will modify the trace element patterns according to the respective element distribution coefficients, and this is discussed below.

The residual, water-free eclogite is then flushed by aqueous fluid released from the hydrous mantle rocks in the peridotite portion of the subducted slab. At this stage, the flushed AOC releases 2 wt% of supercritical liquid at ca. 180 km depth (6 GPa / 1100 °C), beyond the typical source region of arc magmas. This liquid therefore does not induce melting but metasomatises the overlying mantle, which could become an OIB source. Note that without fluid flushing from hydrous mantle devolatilisation, the residual, dry eclogite might simply founder. It is the water from hydrous mantle devolatilisation (breakdown of antigorite, chlorite, or 10 Å phase, depending on slab geotherms; Dvir et al., 2011; Ulmer and Trommsdorff, 1995) that mobilises the incompatible elements from the dry eclogite at the expected conditions above the second critical endpoint of the basalt - water system (Kessel et al., 2005b). Because the resulting liquid is supercritical, element solubilities and thus element mobilities are greatly enhanced, notably for HFSE and LREE (Kessel et al., 2005a). Varying the fluid fractions released from the slab at a given P and T will affect the trace element pattern of the respective sources, much more so when the residual mineral assemblages change, because element mobilities are controlled by the respective fluid - bulk solid element distribution coefficients and mass fractions.

3. Results

3.1. Uranium-Th-Pb systematics

Bulk rock chemical data (Supplementary Table 1) demonstrate that ocean floor serpentinites act as a net sink for seawater-dissolved U, resulting in serpentinite U concentrations of up to 1.25 μg/g. By contrast, Th concentrations are as low as ~0.3 ng/g, i.e., more than two orders of magnitude lower than that of the primitive mantle, reflecting prominent melt depletion of precursor mantle rocks. Pre-serpentinisation U concentrations can thus be estimated to have been as low as ~0.1 ng/g for these samples (using $\kappa_{DMM} = 2.7$). The measured U concentrations are much higher (100 to 1250 ng/g) and translate into hydration-related U enrichments of one to four orders of magnitude. Compared to U, Pb became much less enriched during alteration because Pb has a very low concentration and residence time in the ocean (von Blanckenburg et al., 1996). As a result, the studied serpentinites have extremely high μ values of up to 2100, and κ- and ω ($^{232}Th/^{204}Pb$) as low as 0.004 and 0.3, respectively. These values depart dramatically from typical convecting mantle values of ca. 11, 2.7, and 30 (Hart and Staudigel, 1989; White, 2015) but correspond to the range reported for seafloor serpentinites dredged from the Pacific and Indian Oceans (Niu, 2004). The new data confirm that oceanic serpentinites are a major sink for seawater-derived U.

3.2. Lead isotope systematics

The most important aspect of the new dataset is the markedly uranogenic Pb isotope compositions of the serpentinites with $^{206}Pb/^{204}Pb$ ratios approaching 56 (Fig. 1a, Supplementary Table 1). By complete contrast, $^{208}Pb/^{204}Pb$ ratios show no increase with $^{206}Pb/^{204}Pb$ (Fig. 1b), documenting negligible ingrowth of thorogenic Pb since ~120 Ma, and the intercept $^{208}Pb/^{204}Pb \approx 38.3$ is typical for DMM ($37.5 < ^{208}Pb/^{204}Pb < 38.5$; Kramers and Tolstikhin, 1997). To our knowledge, these are the highest $^{206}Pb/^{204}Pb$ ratios so far reported for in-situ altered oceanic lithosphere, along with primitive thorogenic Pb isotope signatures. The discovery of extreme radiogenic Pb ingrowth qualitatively supports the widely accepted model that recycling of seawater derived U plays a central role in the isotopic evolution of the convecting mantle at least since the oxygenation of the atmosphere (the ca. 2.35 Ga Great Oxidation Event, GOE), after which U was selectively lost from the continents (Elliott et al., 1999; Kramers and Tolstikhin, 1997; Kumari et al., 2016).

Forward modelling (Chauvel et al., 1992; Hart and Staudigel, 1989; Stracke et al., 2003) demonstrates that addition of U alone, without further modification of μ and κ in the subduction zone, cannot generate radiogenic Pb isotope compositions of any of the postulated sources of OIB. The new measurements confirm this conclusion. In uranogenic space (Fig. 1a), the slope defined by the serpentinites is far too shallow and does not approach the ca. 1.8 Ga 'apparent age' of the OIB array (Chase, 1981). The misfit in thorogenic space is even more drastic, since the very low ω does not support measurable production of ^{208}Pb (Fig. 1b). In AOC, the relative U enrichment is much more modest than in serpentinites, because oceanic basalt and gabbro have much higher incompatible element concentrations (relative to DMM) prior to hydration. Analysis of Phanerozoic AOC thus provides little insight into the potential Pb-isotope evolution over billions of years, but the 1.9 Ga old oceanic Flin Flon metabasalt data (Babechuk and Kamber, 2011) are more relevant to the OIB discussion. Assuming no modification upon subduction before extended, isolated storage prior to being tapped by partial melting, these ancient AOC samples match the global OIB very well in uranogenic Pb (Fig. 1c; as postulated by Chase, 1981). The thorogenic Pb diagram, however, reveals that the $^{208}Pb/^{204}Pb$ ratios of Flin Flon basalts are far too low for a given $^{206}Pb/^{204}Pb$ ratio when compared to OIB Pb (Fig. 1d), similar to the serpentinites (Fig. 1b), but less extreme.

3.3. Subduction zone modification of Th/U/Pb ratios

The new measurements both from active and ancient ocean floor illustrate that prominent subduction processing of altered oceanic lithosphere and associated fractionation of U/Th/Pb is required, if HIMU

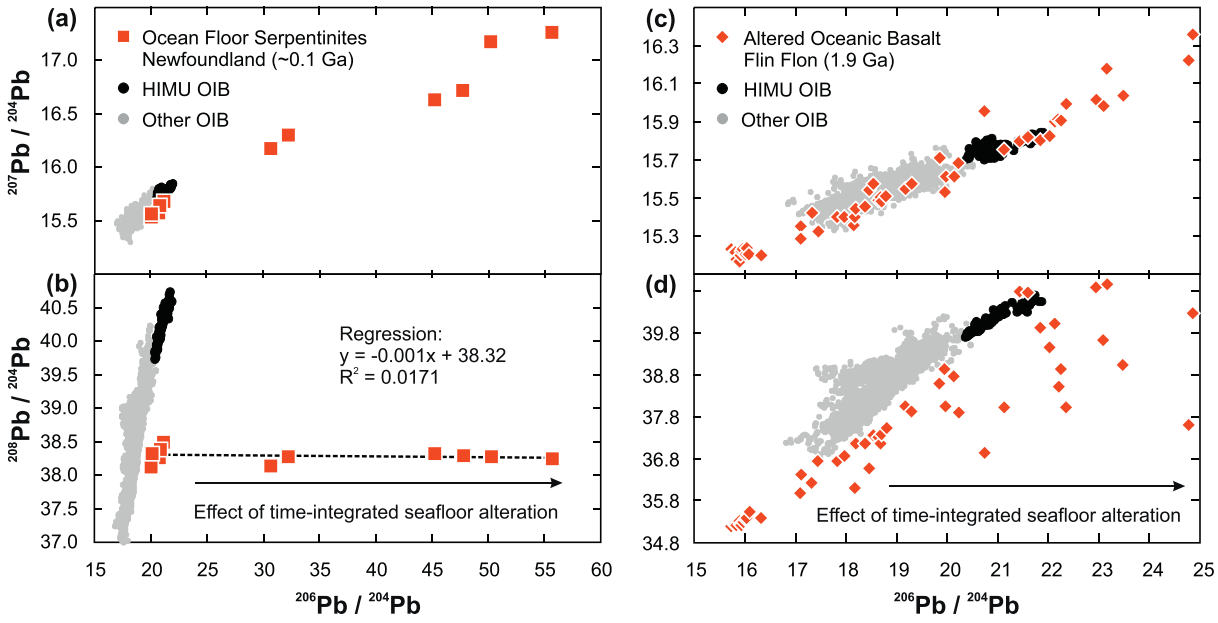

Fig. 1. Measured serpentinite and Palaeoproterozoic AOC Pb isotope compositions. Present day uranogenic (a & c) and thorogenic (b & d) isotope compositions of ca. 100 Ma oceanic serpentinites (a & b; this study) and 1.9 Ga altered oceanic basalts, Flin Flon (c & d; Babechuk and Kamber, 2011), compared to ocean island basalt (OIB) data compilation (Stracke, 2012). HIMU OIB in black, other OIB + MORB in gray (PREMA, EM1, EM2). Note zero slope of thorogenic Pb data of ca. 100 Ma oceanic serpentinites (b).

OIBs are to be sourced from ancient deeply subducted slabs. The prevailing consensus is that excess U entering subduction zones resides in AOC, i.e., in the crustal portion of the slab (Bach et al., 2003; Kelley et al., 2005; Staudigel et al., 1995). Existing models of fluid element mobility with progressive AOC subduction (e.g., Chauvel et al., 1992; Hart and Staudigel, 1989; Kelley et al., 2005; Stracke et al., 2003) attempted to quantify the subduction zone transfer of U, Th, and Pb with the then limited experimental and empirical constraints. More recent and relevant experimental data have highlighted the importance of subduction depth for the relative behaviours of U, Th, and Pb. During early aqueous fluid release (Brenan et al., 1995; Morris and Ryan, 2003; Spandler et al., 2007) up to ca. 70 km depth, Pb transported to subarc depths is released in strong preference over Th and U. This experimental constraint is reflected empirically in the relatively low μ (<9) of average modern continental crust (Kramers and Tolstikhin, 1997) whose ultimate source is the (relatively Pb-rich) fluid-fluxed subarc mantle wedge feeding island arc magmatism. Therefore, partly dehydrated AOC in the forearc to subarc regime will, if anything, have an even higher μ than what entered the subduction zone.

Uranium and Th in the AOC, largely preserved in cool slabs to depths of 120–150 km, will become strongly mobilised along with the remaining Pb, once the aqueous fluids become supercritical liquids at greater depth (Kessel et al., 2005b). Supercritical liquids are characterised by melt-like compositions and, importantly, by preferential Th over U mobility by a factor of up to 2 (Fig. 2). Hence, neither shallow nor deep fluid loss provides the direction of Th/U and U/Pb fractionation required to generate residual AOC with κ >3 that would be a viable source for HIMU OIB (Figs. 1 and 2b). This problem is amplified by the fact that AOC enters subduction with a κ that is already low due to seawater U-metasomatism (Fig. 1d).

In addition to AOC, ocean floor serpentinites also provide a prominent pool of U (but much less so for Th and Pb) for subduction recycling back to the mantle (Kodolányi et al., 2012; Niu, 2004). The limited data on redistribution of U-Th-Pb upon prograde subsolidus mineral transformations in serpentinites suggest that U concentrations remain uniform upon prograde antigorite formation from chrysotile/lizardite, whereas Pb concentrations tend to decrease (Deschamps et al., 2011), and significant Pb is present in the dehydration fluids produced during antigorite breakdown at ca. 60 km depth (Scambelluri et al., 2004). As for AOC, preferential prograde loss of Pb over U and Th is thus indicated. This means that excess U, together with low initial Th and residual Pb concentrations, are transported by serpentinite residues to subarc depths and beyond. Hence, subduction processing of Th-U-Pb cannot lower the μ and increase the κ of serpentinite residues to anywhere near the required values to become sources of OIB.

3.4. Results of Pb isotope ratio forward modelling

Modelling results for dehydrated AOC residue and mantle peridotite metasomatised by supercritical liquids released from subducted slabs are compared and contrasted in Fig. 3. The resulting Pb-isotope evolution over 1.9 Ga shows that a mantle reservoir metasomatised by AOC-derived supercritical slab fluids beyond subarc depth can indeed yield a composition similar to the most radiogenic HIMU OIB for both $^{207}Pb/^{204}Pb$ vs. $^{206}Pb/^{204}Pb$ and $^{208}Pb/^{204}Pb$ vs. $^{206}Pb/^{204}Pb$ (Fig. 3a,b). The misfit in the uranogenic diagram (Fig. 3a) could be eliminated by reducing the time for radiogenic ingrowth from 1.9 Ga by several hundred Ma; easily within the originally envisaged average age range for the HIMU source (Chase, 1981). This illustrates how sensitive the Pb-isotope evolution is to time. The calculations for the complementary dehydrated AOC residue also offer a solution for the uranogenic Pb (Fig. 3c) but fail to reproduce the thorogenic Pb (Fig. 3d), due mainly to the low initial κ, amplified by preferential loss of Th over U to supercritical fluids (Fig. 2b). It may be significant that subtle variations exist in $^{207}Pb/^{204}Pb$ for a given $^{206}Pb/^{204}Pb$ between different HIMU magmatic centres. This could relate to slight variations in age and Th/U/Pb fractionation in the original mantle portions from which basaltic material was extracted paired with differences in P-T and fluid-residue fractions encountered during subduction processing to yield the metasomatised HIMU mantle source.

A further factor could be the initial Pb-isotope composition of the AOC. As mentioned in the description of the modelling parameters, the least-radiogenic known Paleoproterozoic Pb has a higher $^{207}Pb/^{204}Pb$ than the depleted mantle model curve of Kramers and Tolstikhin (1997). The mismatch between model curves and empirical Precambrian data does not exist for the Archean but appears between 2.5 and 1.8 Ga. Kamber (2015) proposed that it could reflect re-fertilization of strongly depleted Archean asthenosphere with more

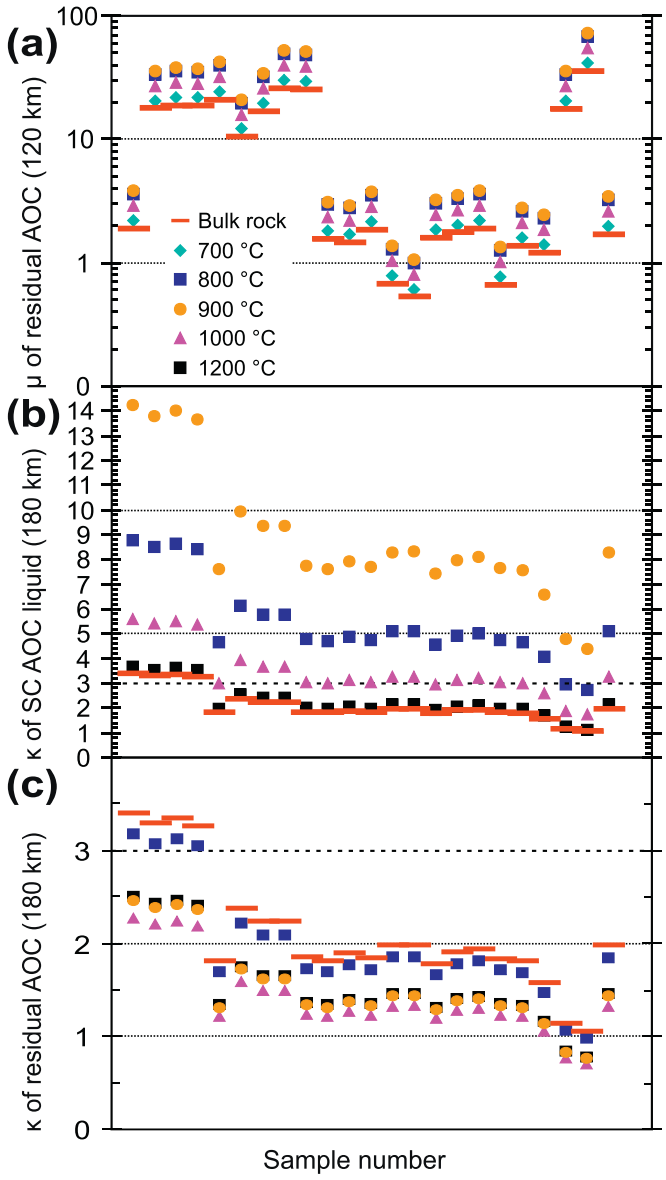

Fig. 2. Results of U-Th-Pb distribution modelling between aqueous fluid, supercritical liquid, and residual basaltic eclogite (dehydrated AOC) at 120 and 180 km depth. The AOC was approximated with 23 empirical Flin Flon hydrated ocean floor basalts spanning the maximum range in U-Th-Pb abundance ratios of the entire data set (data from Babechuk and Kamber, 2011, shown across horizontal axis), to mimic demonstrated variation in AOC composition (compare e.g., AOC Super Composites 504, 801, 417/418; Bach et al., 2003; Kelley et al., 2003; Staudigel et al., 1995). Residual AOC composition after subcritical aqueous fluid extraction of 5 wt% at 120 km (4 GPa) and 2 wt% supercritical liquid at 180 km (6 GPa) modelled with liquid-eclogite partition coefficients of Kessel et al. (2005a, their supplementary table 5) as explained in the main text. Predicted μ signatures ($^{238}U/^{204}Pb$) in (a) AOC eclogite residue at 120 km depth following aqueous fluid extraction, and (b) κ ($^{232}Th/^{238}U$) of supercritical liquid and (c) residual AOC, respectively, at 180 km depth. Dashed line at $\kappa = 3$ represents the minimum value required for generating HIMU-OIB-compatible Pb isotope signatures from Flin Flon AOC material within 1.9 Ga.

fertile lower mantle material during an end-Archaean mantle reorganisation event. AOC formed over 2.5 and 1.8 Ga age interval could therefore have variable initial $^{207}Pb/^{204}Pb$, which might also be reflected in HIMU.

Models performed with AOC Super Composite data for Sites 801 and 504 are broadly consistent with these findings but clearly yielded an overall poorer match (Supplementary Information 2). None of the model results for AOC Site 504 Super Composite data can account for the HIMU source Pb isotopic signatures. For AOC Site 801 Super Composite data, uranogenic Pb isotope systematics are compatible with both HIMU source proposals, i.e., metasomatised mantle peridotite and residual AOC. However, neither model provides a solution for thorogenic Pb, because the final $^{208}Pb/^{204}Pb$ is, again, too low for a given $^{206}Pb/^{204}Pb$. Note that modern MORB has elevated U concentrations due to extraction from U-enriched modern mantle; hence, unaltered modern MORB κ values are lower than those of Proterozoic MORB, a fact that was not corrected for in the current models.

3.5. Model results for extended trace element subduction processing

Finally, the new HIMU source model was tested by comparing its predicted extended trace element systematics with those of observed HIMU basalts. The evolution of slab surface temperatures with progressive subduction (after Fig. 6 of Syracuse et al., 2010) informed the envisaged two-stage dehydration history in the slab: (1) direct dehydration of AOC at 4 GPa /800 °C (120 km depth) and; (2) expulsion of supercritical liquid at 6 GPa / 1100 °C, induced by aqueous fluid from dehydrated serpentinite infiltrating the dehydrated AOC. The inset in Fig. 4 portrays the signature of dehydrated AOC residue at 4 GPa, illustrating the loss of ca. 50% Pb but with the Th/U ratio remaining unchanged. In strong contrast, the supercritical liquid released at 6GPa / 1100 °C experienced Th-U fractionation, with Th being significantly more mobile than U. With increasing temperature, the difference in mobility between Th and U decreases (compare Fig. 2b). The signature of modelled supercritical liquid release from AOC beyond subarc depths at 180 km (Fig. 4 inset) broadly resembles the trace element pattern for HIMU OIB (Jackson et al., 2015; Stracke, 2012), notably when mixing of the metasomatised source with the so-called prevalent mantle component (PREMA, Zindler and Hart, 1986), or with DMM, is included (e.g., Kamber and Collerson, 1999), as indicated by the tight arrays of HIMU OIB Pb-isotopes (Fig. 3a,b).The modelled positive Sr anomaly is the combined result of moderate mobility at 800 °C/4 GPa with near complete mobility at 1100 °C/6 GPa. Absence of a negative Nb-Ta anomaly indicates that rutile was not stable in the residual eclogite. This suggests temperatures above 1000 °C (6 GPa) according to the element mobility data in Kessel et al. (2005a).

4. Discussion

4.1. A four-stage model for the HIMU OIB source

Our preferred model for the HIMU OIB source involves a four-stage evolution, which is illustrated in Fig. 4 and combines many previously proposed concepts (Halliday et al., 1992; Li et al., 2014; Niu and O'Hara, 2003; Weiss et al., 2016).

Stage 1 encompasses post-GOE seawater-alteration of oceanic lithosphere, producing AOC and serpentinite (Nr. 1 in Fig. 4), each with their characteristic trace element abundance patterns, including prominent U enrichment.

Subduction of oceanic lithosphere induces fluid removal and element recycling into arc magmas (**Stage 2**), depleting the slab (at Nr. 2 in Fig. 4) primarily in water, large ion lithophile elements (LILE), and Pb, elevating the U/Pb ratio of AOC even higher, also increasing Th/Pb, but not significantly affecting Th/U (AOC eclogite 4/800 in Fig. 4 inset). It is this early aqueous fluid loss from slab that can account for the apparent depletion in LILE and K characteristic of some OIBs including HIMU, thus suggesting that K-mica is not an important residual phase in the subducted lithologies at this stage (see further discussion below).

Stage 3 occurs at depths beyond the subarc region, where aqueous fluids liberated from hydrous, serpentinited peridotite (dehydration of antigorite, chlorite, or 10 Å phase; Schmidt and Poli, 2014) percolate into, and equilibrate with, basaltic eclogite residues (the AOC generated in Stage 2) to generate a supercritical liquid (6/1100) at Nr. 3 in Fig. 4. This step is conceptually similar to the model of Spandler and Pirard (2013). Note that cool hydrous mantle rocks from slab interiors

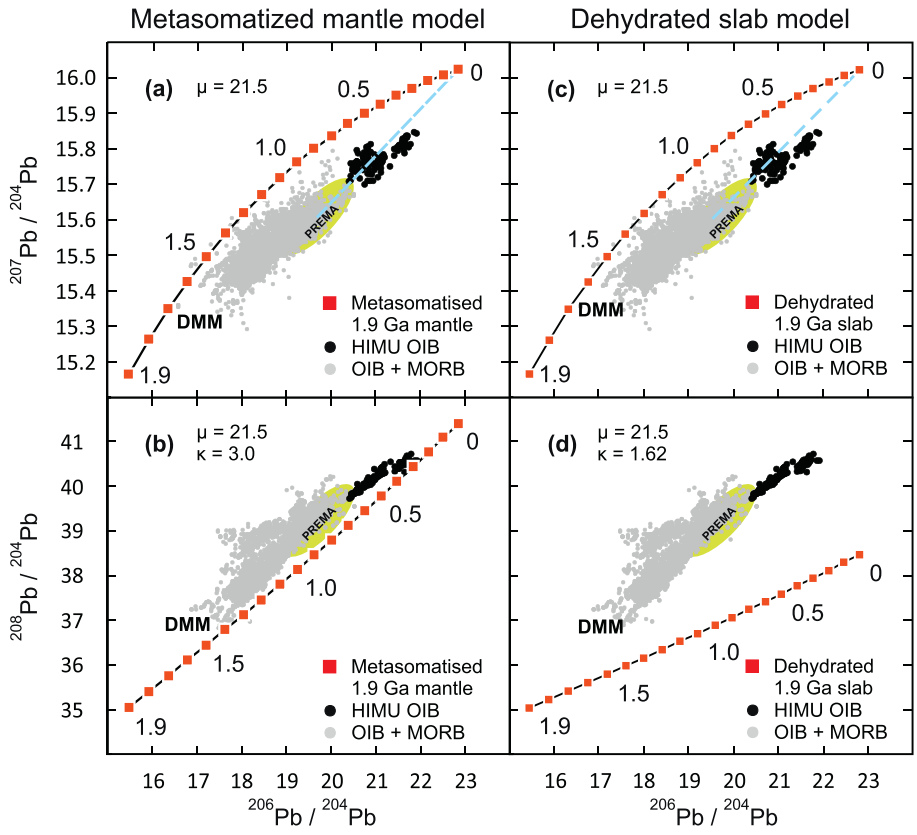

Fig. 3. Pb isotope evolution forward modelling results. Comparison of observed OIB data (HIMU in black, other OIB + MORB in gray) with forward model calculations (shown from 1.9 to 0 Ga in 0.1 Ga increments, labelled; $\mu = {}^{238}U/{}^{204}Pb$, $\kappa = {}^{232}Th/{}^{238}U$) in uranogenic (a & c) and thorogenic (b & d) Pb isotope space. Results represent evolution of modified AOC (modelled from average Flin Flon data with predicted fluid - residue element distributions at 120 and 180 km depth; for details refer to main text). Mantle metasomatised by AOC-derived supercritical liquid (a) and the dehydrated AOC residue (c) models both evolve to sufficiently radiogenic compositions. Less radiogenic compositions could be produced by admixing PREMA or DMM in the plume conduit (dashed blue lines projecting to PREMA/DMM). In thorogenic Pb isotope space only the metasomatised mantle model (b) generates the necessary high $^{208}Pb/^{204}Pb$ ratios. The dehydrated slab model (d) evolves to too low $^{208}Pb/^{204}Pb$ ratios for any of the four principal OIB sources. Field for PREMA after Stracke (2012).

(e.g., formed upon slab bending; Ranero et al., 2003) host the largest fraction of water at these depths (Schmidt and Poli, 2014). The resulting solute-rich supercritical liquids, which are characterised by variable enrichments in incompatible elements and light rare earth elements (LREE), are highly mobile at these P-T conditions (Kessel et al., 2005a), leaving the slab to fertilise ambient asthenospheric peridotite. This imparts characteristic trace element signatures including the high U/Pb, Th/Pb and elevated but still low Th/U to convecting supra-subduction zone mantle (green-blue region in Fig. 4). Although U enrichment (relative to Th and Pb) in oceanic serpentinites can be extreme, the net amount of U transport in aqueous fluid from dehydrating slab mantle serpentinite likely only accounts for a few percent of the total U budget of the supercritical liquid escaping the slab; hence, for Pb-isotope models, serpentinite-derived U is not highly relevant (see also below). By contrast, the key is that serpentinite dehydration triggers element transport out of the basaltic slab portion via a supercritical metasomatic agent (Supercritical Liquid 6/1100 in Fig. 4 inset). These fluids yield a modelled PM-normalised trace element pattern with many features observed in HIMU OIB (e.g., from Tuvalu and St. Helena; at Nr. 4 in Fig. 4), distinctly different from the initial pattern of the AOC composite (Fig. 4 inset). Mantle domains re-fertilised by such supercritical liquids can have two fates as they are transferred into the convecting mantle. First, they can be effectively mixed into depleted asthenosphere and contribute to the element budget and isotope ratio characteristics of DMM. Second, those for which stirring did not result in effective mixing will evolve and age over hundreds of millions of years to generate the time-integrated Pb isotopic signatures characteristic of the HIMU OIB source. Whether such discrete metasomatised mantle source regions persist as domains in the convecting mantle (Tackley, 2000), reside in the lower lithospheric mantle (Halliday et al., 1992; Pilet et al., 2008; Van Keken et al., 2002; Weiss et al., 2016), or are located peripheral to subcontinental lithospheric mantle (Weiss et al., 2016) is a geodynamically interesting question but not critical for the present study.

Finally, **Stage 4** involves plume initiation, possibly in thermochemical piles at the core-mantle boundary (White, 2015) that host ancient subducted slab residues (possibly Neoarchaean; Cabral et al., 2013). Fluid-metasomatised mantle source regions with HIMU flavour are then entrained by the plume en route to the surface, either during upwelling or from previously foundered subcontinental lithospheric mantle (SCLM) portions (Weiss et al., 2016), and the resulting melt at upper mantle levels (compare White, 2015) will carry the diagnostic Pb-isotope composition of mixing between HIMU and DMM source components.

4.2. Model-independent, additional, relevant observations

It is recognised that extrapolation of experimental data to predict U/Th/Pb behaviour in natural oceanic slabs carries a large uncertainty, and that additional information is required to assess the plausibility of the proposed model. First, while trace element patterns of any published AOC Composite (Bach et al., 2003; Kelley et al., 2005; Staudigel et al., 1995) strongly contrast the homogeneous pattern reported for HIMU OIB, the model composition of mantle portions metasomatised by supercritical liquids derived from AOC share several elemental characteristics with it (Fig. 4 inset). Agreement is evident for the prominent LREE

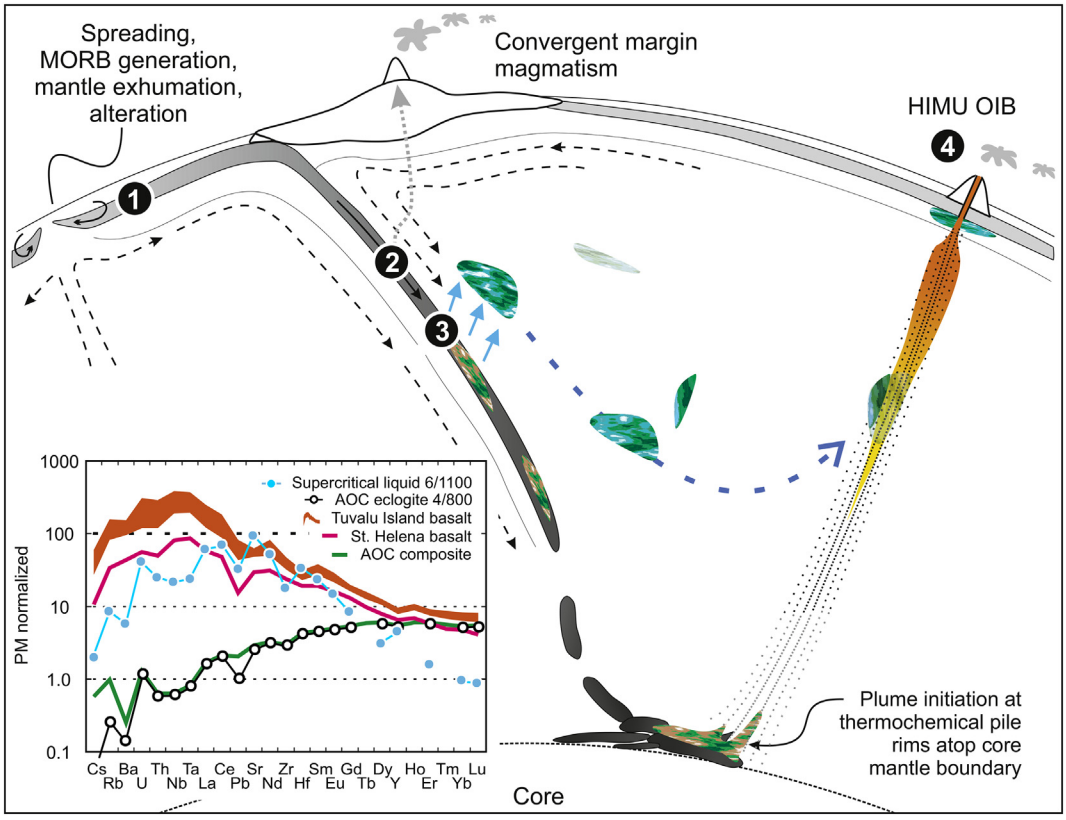

Fig. 4. Illustration of the preferred model for HIMU OIB genesis in 4 stages (white numbers in black circles). The trace element pattern inset illustrates limited element loss from AOC (AOC composite 504B; Bach et al., 2003) upon dehydration at subarc depths (at 4 GPA / 800 °C). Central to this model is that metasomatism of convecting mantle to generate the HIMU OIB source occurs beyond subarc depth via supercritical liquid liberated from the down going slab (at 6 GPa/1100 °C) that had earlier lost Pb along with LILE (i.e., the "arc magmatism Pb shortcut"; gray dotted arrow) and experienced a relative enrichment in Th over U (compare PM-normalised U and Th for the starting AOC and the supercritical liquid at 6/1100). We favour the scenario where dehydration of former serpentinites releases aqueous fluids relatively enriched U (but still with low concentrations) but otherwise low trace element abundances that then interact with basaltic eclogite residue to generate supercritical liquid prominently enriched in incompatible trace elements.

enrichments combined with a relative depletion in LILE and Pb, inherited from aqueous fluid loss having occurred earlier at shallower subduction levels. Differences between modelled and observed patterns, notably for the incompatible elements, largely mirror those inherited from the initial compositions of selected AOC. The model calculations (not shown) using the Site 801 Super Composite (Kelley et al., 2003) and the Flin Flon basalts (Babechuk and Kamber, 2011) as AOC are similar to a first order to the example shown in Fig. 4 inset.

Compositional variation of the mobile phase escaping the subducting slab is generated in response to changes in (i) the residual slab mineralogy, particularly when specific accessory phases appear or disappear (compare e.g., Spandler et al., 2003), (ii) P-T of slab dehydration, and (iii) the fractions of fluid / supercritical liquid escape. A relevant observation is that strongly altered AOC has elevated K_2O concentrations (Bach et al., 2003; Kelley et al., 2003) which can stabilise phengite (Schmidt et al., 2004) in residues like those modelled here, i.e. at ~180 km depth (6 GPa/1200 °C). If the mode of phengite is below a few percent, this phase can be completely dissolved by the percolating fluid (Schmidt et al., 2004). In this case, our model for subduction processing correctly predicts the composition of the supercritical liquid leaving the slab. By contrast, for more K-rich compositions, some of the phengite may remain stable in the residual mineral assemblage, and retain significant fractions of Ba, Rb, Cs, Nb, and Ti. This is seen empirically in phengite-garnet-clinopyroxene-spinel±carbonate veins within garnet peridotite equilibrated at ca. 180 km depth (Scambelluri et al., 2008). Because HIMU compositions do not show relative depletions in the elements discussed (compare trace element pattern for the supercritical liquid in Fig. 4 inset), it is concluded here that phengite is not important in the genesis of the HIMU source.

Several authors have argued that the Nb-Ta-Th-U systematics of OIBs in general, not just of the HIMU type, are incompatible with a dehydrated slab AOC source origin (e.g., Kamber and Collerson, 2000; Rudnick et al., 2000; Stracke, 2012). Based on Nb/Ta systematics, Rudnick et al. (2000) concluded (p. 280) that "the amount of refractory eclogite in the OIB source is small". The HIMU OIB of the Cook-Austral chain (Hanyu et al., 2011) has Nb/U ratios lower than MORB (ca. 44 versus 50) and Nb/Th much lower than MORB (ca. 12 versus 18). This observation again supports preferential Th over Nb addition via a U-enriched component to the HIMU source region, plausibly achieved via supercritical liquid metasomatism of ambient mantle rocks. Moreover, conspicuously low Ba/Nb in HIMU magmas (Willbold and Stracke, 2006) can readily be accounted for via subduction processing, i.e., earlier Ba loss via aqueous fluid dehydration, as also shown for Pb (illustrated in Fig. 4 inset).

All HIMU OIB data sets tend to have lower LREE but higher HREE compared to modelled supercritical liquid derived from AOC. This could be achieved if the fluids metasomatised relatively HREE-enriched PREMA and/or DMM to form the HIMU OIB source signature. We note that this kind of mixing is consistent with the HIMU uranogenic Pb-isotope arrays (Fig. 3). An attractive aspect of a HIMU source fertilised by mantle metasomatism via supercritical liquid is that the resulting composition is enriched in incompatible elements, partial melting of which can generate characteristic HIMU trace element patterns at plausible melting fractions. By contrast, melt fractions required to derive HIMU basalt with observed trace element patterns from partial melting of residual AOC eclogite are problematically low. In fact, the geochemical trends predicted by our model of mantle metasomatism might even account in part for continental intraplate magmatism and possibly even for Group 1 kimberlites (Nowell et al., 2004).

Aqueous fluid liberated directly from the subducted hydrous mantle peridotite via devolatilisation (stage 3 of our model), has modest capacity to transport U and is not relevant for Th and Pb because the initial concentrations of Pb and Th are so low (Supplementary Table 1). Thus, the slab peridotite fluid contribution to the bulk of U in the supercritical liquid liberated from AOC eclogite would only ever be subordinate and result in U/Th ratio variability within the noise of variability inherited from ocean floor alteration of the AOC. Moreover, the pattern of aqueous fluid element mobility at ca. 180 km depth in equilibrium with residual garnet peridotite is expected to be largely comparable to that for the K-free basalt-water system (Kessel et al., 2005a). Consequently, subduction processing of the hydrous peridotite component is expected to cause non-resolvable geochemical effects in the overall subduction processing model presented here.

Growing consensus is emerging that OIBs of different isotopic character also possess distinctive major element compositions. In this regard, HIMU magmas stand out as being quite alkaline and magnesian with elevated CaO/Al_2O_3 (Jackson and Dasgupta, 2008; Weiss et al., 2016). Such characteristics argue against an origin from basaltic eclogite melting (i.e., the subducted AOC residue) but suggest that HIMU OIB are more likely sourced from garnet peridotite (e.g., Herzberg et al., 2014) metasomatised by a supercritical liquid as proposed here.

The four-stage model presented here is consistent with constraints from time-integrated radiogenic isotope ratio characteristics other than Pb. The non-radiogenic $^{87}Sr/^{86}Sr$ (<0.703), within a narrow range for a given, intermediate $^{143}Nd/^{144}Nd$ (Stracke, 2012), is consistent with a low Rb/Sr and elevated Sm/Nd of the proposed metasomatising agent, since the supercritical liquids in equilibrium with garnet are prominently HREE depleted and the slab has lost a large fraction of Rb during earlier dehydration (Fig. 4 inset). Conspicuously low $^{176}Hf/^{177}Hf$ ratios for a given $^{143}Nd/^{144}Nd$ of HIMU relative to other oceanic basalts (Salters and White, 1998; Stracke, 2012) are consistent with the much higher mobility of Hf relative to Lu in supercritical liquids in equilibrium with a garnet-bearing residue (Kessel et al., 2005a). For lack of experimental data on fluid mobility at UHP conditions, no constraints can be given for Os isotope systematics. We note that Re/Os can be markedly elevated in ocean floor basalt through oxidative alteration (Site 801; Reisberg et al., 2008) and that Re can also be enriched in serpentinites (Tsuru et al., 2000); hence, the moderately radiogenic Os isotope ratios of HIMU (e.g., Hanyu et al., 2011) seem permissible within available constraints.

4.3. Age and spatial distribution of the HIMU source

The strong element fractionation imparted by dehydration-related supercritical liquids can establish the observed time-integrated radiogenic isotope ratios of HIMU OIBs, notably Pb isotope systematics, over much shorter time-scales than billions of years (e.g., Halliday et al., 1995). The HIMU-like source signature could thus be a rapidly evolved feature within metasomatic mantle lithosphere, formed as recently as during the Mesozoic (McCoy-West et al., 2016; Scott et al., 2016). McCoy-West et al. (2016) suggested that young, carbonatite-related radiogenic Pb signature with extreme $^{238}U/^{204}Pb$ and $^{232}Th/^{204}Pb$, which is widely observed in the southwest Pacific, may reflect a secular change in mantle chemistry consistent with the increased prevalence of carbonatite sources (of unconstrained origin) during the Phanerozoic. Carbonatitic fluids have been proposed as a possible metasomatising agent in the HIMU source (compare Castillo, 2015; Jackson and Dasgupta, 2008; Weiss et al., 2016).

In this context, it is important to consider the limits imposed by Sr isotope constraints. Post-2 Ga marine $^{87}Sr/^{86}Sr$ ratios are quite radiogenic and exceed 0.704 (e.g., Shields and Veizer, 2002), higher than the upper limit of HIMU OIBs (0.703). This means that if there was a marine carbonate component in the HIMU source it would have to have been Archaean in age (as acknowledged by Castillo, 2015). A > 2.35 Ga age for at least some of the HIMU source could be supported by mass independent isotope fractionation (MIF) of S in Mangaia HIMU lavas (Cabral et al., 2013). However, there is a paucity of carbonate in the Archaean sedimentary record (likely due to the high Fe-content of Archaean seawater inhibiting calcite crystallisation; Sumner and Grotzinger, 1996). It is also worth recalling that it is difficult, if not impossible, to arrive at present-day HIMU OIB Pb-isotope ratios with starting compositions that are much older than 2 Ga because the resulting $^{207}Pb/^{204}Pb$ ratios become too high.

Furthermore, there is wide agreement that it was the post-Archaean preferential U transfer that played a critical role in producing the HIMU source. The relatively non-radiogenic Sr isotopes could alternatively be explained as reflecting admixture from DMM component ($^{87}Sr/^{86}Sr <$ 0.703) dominating the Sr signature of HIMU OIBs. If the bulk of the HIMU source (including its Pb) is post-Archaean, the S MIF observation from Mangaia could represent storage of a minor OIB component at great depth (e.g., in the thermochemical pile). The MIF S isotope signal is not found in all HIMU locations (e.g., Labidi et al., 2014) but ^{33}S-deficient S has been reported from some EM1 OIBs (Delavault et al., 2016). Archaean recycled S could thus be from material of the thermochemical pile at the base of the plume (e.g., Farquhar and Jackson, 2016), which could become incorporated into the HIMU source during mixing with a younger, foundered metasomatic mantle portion, or into HIMU source regions during plume upwelling. Alternatively, the MIF S signal in OIBs could have an origin unrelated to the recycling of surficial S (e.g., Labidi et al., 2013).

Accepting that multiple sources contribute to the diverse OIB types, the more fundamental question of their relative contributions to the HIMU magma emerges. Our model in Fig. 4 involves material from the thermochemical pile, metasomatised mantle, and PREMA or DMM, unless this last component already forms an integral part of the metasomatised mantle component.

In addition to evidence supporting the metasomatic HIMU OIB genetic model, the rare occurrence itself of the HIMU source component may be relevant. Because serpentinites abundantly form in slow-spreading oceanic settings (see discussion in Alt et al., 2013), HIMU OIB source generation by the process proposed here may have occurred predominantly during subduction of such cold lithosphere in response to specific stages of plate reorganisation on Earth. Episodic subduction of slow-spreading, cold, oceanic lithosphere poor in sediment since the Proterozoic may be a possible reason for the rarity of HIMU OIB magmas. The fact that slow-spreading oceanic lithosphere is cold when it eventually subducts may be a decisive factor. Along comparatively cool subduction trajectories, the hydrous mantle minerals antigorite and phase A in the cooler interior of the subducting slab remain stable to depths exceeding 200 km (Fumagalli and Poli, 2005; Syracuse et al., 2010). For cases where the aqueous fluid interacts with sediment to form a supercritical liquid, an EM1 type source might be formed, blurring and overwhelming the HIMU-type U-Th-Pb abundance ratios. Close spatial association between HIMU and EM1 type sources is documented for the Cook-Austral islands (e.g., Jackson et al., 2015) and suggests that slab fluid percolation is non-pervasive; thus producing metasomatised mantle domains of different flavour and limited spatial extent.

5. Recycling of U into the asthenosphere

Because survival of a pure HIMU mantle source is rare, the magnitude and impact of U recycled to the convecting mantle via subduction of hydrous mantle rocks (serpentinites) since the GOE ca. 2.35 Ga ago (Holland, 1984) needs to be explored. It should be noted that uncertainty still remains regarding ventilation of the deeper ocean after the GOE, but an oxygenated deep ocean is not a pre-requisite for models similar to the one advanced here. Namely, the key process is the delivery of U from the continents to the ocean via weathering, and sequestering of marine U into the seafloor, which can proceed under different redox conditions (Arnold et al., 1998; Singer et al., 2009). In this regard,

the fact that the 1.9 Ga Flin Flon AOC has evolved to very radiogenic Pb-isotope compositions is crucial, because it shows that by that time, marine U was effectively transferred into altered ocean floor. The following mass balance is based on the estimate of subduction recycled U required to generate the present-day κ ($^{232}Th/^{238}U$) of the DMM of 2.5 while maintaining a time-integrated $\kappa_{Pb(DMM)}$ of ca. 3.7 (Elliott et al., 1999), thus offering a successful solution to the second terrestrial Pb-isotope paradox. These authors concluded that some 2.5 $*10^9$ g/a of "excess" U may have been recycled back into the convecting mantle. The purpose of our mass balance is to explore what fraction of this excess U may be provided by serpentinite subduction.

The average U concentration of serpentinite of our data is 0.7 μg/g (Supplementary Table 1). Assuming that all excess U that was subducted (i.e., $2.5 * 10^9$ g/a) originated from serpentinites, $4 * 10^{15}$ g/a serpentinite subduction is required. At a density of serpentinite of 2.7 g/cm^3, this translates into $1.3 * 10^{15}$ cm^3 or 1.3 km^3. The mean oceanic plate production is estimated (Parsons, 1982; Rowley, 2002) to 3.4 km^2/a, also representing a reasonable estimate for how much oceanic lithosphere is subducted per year. Assuming a partially hydrated oceanic plate thickness of 10 km, about 4% of serpentinite of the Newfoundland-type presented here would be required to provide all excess U subducted to the mantle per year. This simple calculation demonstrates the potential importance of oceanic serpentinites as U carriers into the convecting mantle and its relevance to solutions for the second terrestrial Pb-isotope paradox. The uncertainties of the mass balance estimate are arguably large and include:

(1) The depth of U-enrichment. It can be reasoned that the several orders of magnitude U enrichment during serpentinisation reported here and by others (e.g., Andreani et al., 2014; Boschi et al., 2013; Kodolányi et al., 2012; Niu, 2004; Paulick et al., 2006) may not reach depths exceeding about 40–60 m below seafloor (Kodolányi et al., 2012; Paulick et al., 2006), despite serpentinisation itself reaching as far as 20 km down into the oceanic lithosphere (Ranero et al., 2003). If true, this would imply that the uppermost 60 m of igneous oceanic lithosphere should be comprised of 2/3 serpentinite to provide $2.5 * 10^9$ g/a of U. This is certainly too much for fast spreading regimes but might be attained in slow spreading environments. Note, however, that Bach et al. (2003) reported hydration-related U enrichments in basaltic rocks to depths of up to 700 m; hence, hydration-related U enrichment in serpentinites might also extend much deeper;

(2) The mass of serpentinite entering subduction zones. Neither the fraction of serpentinite in an oceanic slab, nor the depth of serpentinisation by oxidised seawater within the slab are well known. Estimates of serpentinisation of subducting oceanic lithosphere are as high as 15–20% in the uppermost 20 km of the subducting mantle below the Chile trench (Ranero and Sallares, 2004). Other estimates of the fraction of serpentinites are 5–10% for slow-spreading oceanic lithosphere (Alt and Shanks, 2003; Dick, 1989), and 3–5% of the total oceanic crust (compiled in Alt and Shanks, 2003). However, serpentinisation occurs at depth in places where none is exposed at the seafloor (Alt and Shanks, 2003), suggesting that 3% serpentinised peridotite in the total oceanic crust should be considered a minimum estimate;

(3) The extent of preservation of serpentinite-bound U in the slab during progressive subduction. By analogy with AOC (Kessel et al., 2005a, 2005b), significant fractions of U can be expected to remain compatible in the hydrated DMM portion of the slab to the point where a supercritical fluid is liberated. In the simple MgO-SiO_2-H_2O (MSH) system, the second critical endpoint occurs at depths of over 300 km (Melekhova et al., 2007). For natural hydrated DMM compositions, the second critical endpoint is shallower but still beyond that determined for the basalt-water system (Kessel et al., 2005b). Therefore, subduction of former oceanic serpentinites represents a mechanism of transferring seawater-derived U to depths well beyond the subarc, where the residual excess U can eventually be resorbed into the convecting mantle;

(4) Average AOC contributes excess U to subduction zones and there may be no need for additional serpentinite-hosted U. However, the net AOC contribution to U recycling is also poorly constrained. Estimates for κ values of AOC composites range by one order of magnitude, between 2.0 and 0.2 (e.g., Bach et al., 2003; Hart and Staudigel, 1989; Kelley et al., 2005) and encompass different sections (i.e., thicknesses) of the basaltic crust. Importantly, it seems that U enrichment in AOC is largely confined to the pillow basalt section (Bach et al., 2003; Hart et al., 1999). Staudigel et al. (1995) estimated U addition to subduction zones by AOC to be of the order of 10^9 g/a (derived from $0.3 * 10^9$ g/a U addition to each km^2 of the upper 500 m of oceanic crust for their AOC super-composite). If this is correct, the amount of serpentinite-derived U could actually dominate the subduction recycling flux, unless there is another yet unknown flux of U back to the convecting mantle;

(5) Neither of the above estimates takes into account the amount of U delivered to subduction by sediments. We note that clastic sediments are characterised by a deficit in U relative to Th due to U removal during continental weathering at least since the GOE. Unless the U/Th ratio of residual sediment becomes prominently increased during progressive subduction (which is unlikely in view of experimental data), addition of a sediment component to the convecting mantle seems to counteract excess U recycling by serpentinites and AOC.

Considering the five points above, there are two main uncertainties regarding the role of oceanic serpentinite as a U carrier to the mantle. The first is the degree and depth to which U enrichment progressed during ocean floor hydration. The second is the exact nature of U/Th/Pb fractionation and fluid/residue evolution of hydrated ultramafic rocks during subduction zone processing. Notwithstanding these uncertainties, our first-order mass balance suggests that transport of U in subducted serpentinite can make a significant contribution to U recycling, potentially even dominating the total net U-addition to the post-Archaean convecting mantle.

The greatest proportion of recycled U falls victim to cryptic metasomatism in the convecting mantle, which is the expected result of homogenisation of residual peridotitic slab materials or metasomatised domains and ambient mantle by efficient mixing (Tackley, 2000). Residual peridotite that completely dehydrated prior to reaching supercritical liquid stability (typical of intermediate to warm slab geotherms) may be particularly effective in conveying such surface U to the deep mantle. Over the last 2 billion years, this has reduced the modern MORB source Th/U ratio from 4 to 2.6 (e.g., Kamber and Collerson, 1999) and has led to an accelerated evolution of the DMM $^{206}Pb/^{204}Pb$ along with a slowdown in $^{208}Pb/^{204}Pb$. These observations constitute the second terrestrial Pb paradox (e.g., Kramers and Tolstikhin, 1997), also known as the kappa conundrum (Elliott et al., 1999), and highlight the importance of serpentinisation by seawater for planetary-scale differentiation.

Supplementary data to this article can be found online at https://doi.org/10.1016/j.lithos.2018.07.010.

Acknowledgments

We are grateful for the thoughtful reviews of A. Stracke and D. Murphy that helped to clarify some aspects of the presentation. This research used samples provided by the Deep Sea Drilling Project and Ocean Drilling Program, which are sponsored by funding agencies of the participating countries under management of Joint Oceanographic

Institutions (JOI), Inc. The project was supported by the Swiss National Science Foundation (Grant number PP002-106569 to TP).

References

Alt, J.C., Schwarzenbach, E.M., Frueh-Green, G.L., Shanks, W.C., Bernasconi, S.M., Garrido, C.J., Crispini, L., Gaggero, L., Padron-Navarta, J.A., Marchesi, C., 2013. The role of serpentinites in cycling of carbon and sulfur: Seafloor serpentinization and subduction metamorphism. Lithos 178, 40–54.

Alt, J.C., Shanks, W.C., 2003. Serpentinization of abyssal peridotites from the MARK area, Mid-Atlantic Ridge: Sulfur geochemistry and reaction modeling. Geochimica et Cosmochimica Acta 67, 641–653.

Andersen, M.B., Elliott, T., Freymuth, H., Sims, K.W.W., Niu, Y.L., Kelley, K.A., 2015. The terrestrial uranium isotope cycle. Nature 517, 356–U463.

Andreani, M., Escartin, J., Delacour, A., Ildefonse, B., Godard, M., Dyment, J., Fallick, A.E., Fouquet, Y., 2014. Tectonic structure, lithology, and hydrothermal signature of the Rainbow massif (Mid-Atlantic Ridge 36 degrees 14' N). Geochem. Geophys. Geosyst. 15, 3543–3571.

Arnold, T., Zorn, T., Bernhard, G., Nitsche, H., 1998. Sorption of uranium(VI) onto phyllite. Chemical Geology 151, 129–141.

Babechuk, M.G., Kamber, B.S., 2011. An estimate of 1.9 Ga mantle depletion using the high-field-strength elements and Nd-Pb isotopes of ocean floor basalts, Flin Flon Belt, Canada. Precambrian Research 189, 114–139.

Bach, W., Alt, J.C., Niu, Y.L., Humphris, S.E., Erzinger, J., Dick, H.J.B., 2001. The geochemical consequences of late-stage low-grade alteration of lower ocean crust at the SW Indian Ridge: Results from ODP Hole 735B (Leg 176). Geochimica et Cosmochimica Acta 65, 3267–3287.

Bach, W., Peucker-Ehrenbrink, B., Hart, S.R., Blusztajn, J.S., 2003. Geochemistry of hydrothermally altered oceanic crust: DSDP/ODP Hole 504B - Implications for seawater-crust exchange budgets and Sr- and Pb-isotopic evolution of the mantle. Geochemistry Geophysics Geosystems 4 art. no.-8904.

Boschi, C., Bonatti, E., Ligi, M., Brunelli, D., Cipriani, A., Dallai, L., D'Orazio, M., Fruh-Green, G.L., Tonarini, S., Barnes, J.D., Bedini, R.M., 2013. Serpentinization of mantle peridotites along an uplifted lithospheric section. Mid Atlantic Ridge at 11 degrees N. Lithos. Vol. 178 pp. 3–23.

Brenan, J.M., Shaw, H.F., Ryerson, F.J., 1995. Experimental-Evidence for the Origin of Lead Enrichment in Convergent-Margin Magmas. Nature 378, 54–56.

Cabral, R.A., Jackson, M.G., Rose-Koga, E.F., Koga, K.T., Whitehouse, M.J., Antonelli, M.A., Farquhar, J., Day, J.M.D., Hauri, E.H., 2013. Anomalous sulphur isotopes in plume lavas reveal deep mantle storage of Archaean crust. Nature 496, 490–493.

Castillo, P.R., 2015. The recycling of marine carbonates and sources of HIMU and FOZO ocean island basalts. Lithos 216, 254–263.

Chase, C.G., 1981. Oceanic island Pb - 2-stage histories and mantle evolution. Earth and Planetary Science Letters 52, 277–284.

Chauvel, C., Hofmann, A.W., Vidal, P., 1992. HIMU EM - The French-Polynesian connection. Earth and Planetary Science Letters 110, 99–119.

Chen, J.H., Edwards, R.L., Wasserburg, G.J., 1986. U-238, U-234 and Th-232 in seawater. Earth and Planetary Science Letters 80, 241–251.

Delavault, H., Chauvel, C., Thomassot, E., Devey, C.W., Dazas, B., 2016. Sulfur and lead isotopic evidence of relic Archean sediments in the Pitcairn mantle plume. Proceedings of the National Academy of Sciences 113, 12952–12956.

Deschamps, F., Guillot, S., Godard, M., Andreani, M., Hattori, K., 2011. Serpentinites act as sponges for fluid-mobile elements in abyssal and subduction zone environments. Terra Nova 23, 171–178.

Dick, H.J.B., 1989. Abyssal peridotites, very slow spreading ridges and ocean ridge magmatism. In: Saunders, A.D., Norry, M.J. (Eds.), Magmatism in the Ocean Basins. Geological Society Special Publication No. 42, pp. 71–105.

Dvir, O., Pettke, T., Fumagalli, P., Kessel, R., 2011. Fluids in the peridotite-water system up to 6 GPa and 800 degrees C: new experimental constrains on dehydration reactions. Contributions to Mineralogy and Petrology 161, 829–844.

Elliott, T., Zindler, A., Bourdon, B., 1999. Exploring the kappa conundrum: the role of recycling in the lead isotope evolution of the mantle. Earth and Planetary Science Letters 169, 129–145.

Farquhar, J., Jackson, M., 2016. Missing Archean sulfur returned from the mantle. Proceedings of the National Academy of Sciences 113 (46), 12893–12895.

Fumagalli, P., Poli, S., 2005. Experimentally determined phase relations in hydrous peridotites to 6.5 GPa and their consequences on the dynamics of subduction zones. Journal of Petrology 46, 555–578.

Halliday, A.N., Davies, G.R., Lee, D.-C., Tommasini, S., Paslick, C.R., Fitton, J.G., James, D.E., 1992. Lead isotope evidence for young trace element enrichment in the oceanic upper mantle. Nature 359, 623–627.

Halliday, A.N., Lee, D.-C., Tommasini, S., Davies, G.R., Paslick, C.R., Fitton, J.G., James, D.E., 1995. Incompatible trace elements in OIB and MORB and source enrichment in the sub-oceanic mantle. Earth and Planetary Science Letters 133, 379–395.

Hanyu, T., Kawabata, H., Tatsumi, Y., Kimura, J.-I., Hyodo, H., Sato, K., Miyazaki, T., Chang, Q., Hirahara, Y., Takahashi, T., Senda, R., Nakai, S., 2014. Isotope evolution in the HIMU reservoir beneath St. Helena: Implications for the mantle recycling of U and Th. Geochimica et Cosmochimica Acta 143, 232–252.

Hanyu, T., Tatsumi, Y., Senda, R., Miyazaki, T., Chang, Q., Hirahara, Y., Takahashi, T., Kawabata, H., Suzuki, K., Kimura, J.I., Nakai, S., 2011. Geochemical characteristics and origin of the HIMU reservoir: A possible mantle plume source in the lower mantle. Geochemistry Geophysics Geosystems 12.

Hart, S.R., Blusztajn, J., Dick, H.J.B., Meyer, P.S., Muehlenbachs, K., 1999. The fingerprint of seawater circulation in a 500-meter section of ocean crust gabbros. Geochimica et Cosmochimica Acta 63, 4059–4080.

Hart, S.R., Staudigel, H., 1989. Isotopic characterization and identification of recycled components. In: Hart, S.R., Gulen, L. (Eds.), Crust/mantle Recycling at Convergence Zones. Kluwer Acad. Publishers, pp. 15–28.

Herzberg, C., Cabral, R.A., Jackson, M.G., Vidito, C., Day, J.M.D., Hauri, E.H., 2014. Phantom Archean crust in Mangaia hotspot lavas and the meaning of heterogeneous mantle. Earth and Planetary Science Letters 396, 97–106.

Holland, H.D., 1984. The chemical evolution of the atmosphere and oceans. Princeton Univ. Press, Princeton, NJ, p. 582.

Jackson, M.G., Dasgupta, R., 2008. Compositions of HIMU, EM1, and EM2 from global trends between radiogenic isotopes and major elements in ocean island basalts. Earth and Planetary Science Letters 276, 175–186.

Jackson, M.G., Koga, K.T., Price, A., Konter, J.G., Koppers, A.A.P., Finlayson, V.A., Konrad, K., Hauri, E.H., Kylander-Clark, A., Kelley, K.A., Kendrick, M.A., 2015. Deeply dredged submarine HIMU glasses from the Tuvalu Islands, Polynesia: Implications for volatile budgets of recycled oceanic crust. Geochemistry Geophysics Geosystems 16, 3210–3234.

Kamber, B.S., 2015. The evolving nature of terrestrial crust from the Hadean, through the Archaean, into the Proterozoic. Precambrian Research 258, 48–82.

Kamber, B.S., Collerson, K.D., 1999. Origin of ocean island basalts: A new model based on lead and helium isotope systematics. Journal of Geophysical Research-Solid Earth 104, 25479–25491.

Kamber, B.S., Collerson, K.D., 2000. Role of 'hidden' deeply subducted slabs in mantle depletion. Chemical Geology 166, 241–254.

Kelley, K.A., Plank, T., Farr, L., Ludden, J., Staudigel, H., 2005. Subduction cycling of U, Th, and Pb. Earth and Planetary Science Letters 234, 369–383.

Kelley, K.A., Plank, T., Ludden, J., Staudigel, H., 2003. Composition of altered oceanic crust at ODP Sites 801 and 1149. Geochemistry Geophysics Geosystems 4.

Kessel, R., Schmidt, M.W., Ulmer, P., Pettke, T., 2005a. Trace element signature of subduction-zone fluids, melts and supercritical liquids at 120-180 km depth. Nature 437, 724–727.

Kessel, R., Ulmer, P., Pettke, T., Schmidt, M.W., Thompson, A.B., 2005b. The water-basalt system at 4 to 6 GPa: Phase relations and second critical endpoint in a K-free eclogite at 700 to 1400 degrees C. Earth and Planetary Science Letters 237, 873–892.

Kodolányi, J., Pettke, T., Spandler, C., Kamber, B.S., Gmeling, K., 2012. Geochemistry of Ocean Floor and Fore-arc Serpentinites: Constraints on the Ultramafic Input to Subduction Zones. Journal of Petrology 53, 235–270.

Kramers, J.D., Tolstikhin, I.N., 1997. Two terrestrial lead isotope paradoxes, forward transport modelling, core formation and the history of the continental crust. Chemical Geology 139, 75–110.

Kumari, S., Paul, D., Stracke, A., 2016. Open system models of isotopic evolution in Earth's silicate reservoirs: Implications for crustal growth and mantle heterogeneity. Geochimica et Cosmochimica Acta 195, 142–157.

Labidi, J., Cartigny, P., Moreira, M., 2013. Non-chondritic sulphur isotope composition of the terrestrial mantle. Nature 501, 208.

Labidi, J., Cartigny, P., Hamelin, C., Moreira, M., Dosso, L., 2014. Sulfur isotope budget (S-32, S-33, S-34 and S-36) in Pacific-Antarctic ridge basalts: A record of mantle source heterogeneity and hydrothermal sulfide assimilation. Geochimica et Cosmochimica Acta 133, 47–67.

Li, M.M., McNamara, A.K., Garnero, E.J., 2014. Chemical complexity of hotspots caused by cycling oceanic crust through mantle reservoirs. Nature Geoscience 7, 366–370.

McCoy-West, A.J., Bennett, V.C., Amelin, Y., 2016. Rapid Cenozoic ingrowth of isotopic signatures simulating "HIMU" in ancient lithospheric mantle: Distinguishing source from process. Geochimica et Cosmochimica Acta 187, 79–101.

Melekhova, E., Schmidt, M.W., Ulmer, P., Pettke, T., 2007. The composition of liquids coexisting with dense hydrous magnesium silicates at 11-13.5 GPa and the endpoints of the solidi in the MgO-SiO_2-H_2O system. Geochimica et Cosmochimica Acta 71, 3348–3360.

Morris, J.D., Ryan, J.G., 2003. Subduction zone processes and implications for Changing composition of the Upper and Lower Mantle. In: Turekian, K.K., Holland, H.D. (Eds.), Treatise on Geochemistry, 1st Edition Vol. 2, pp. 451–470.

Nebel, O., Arculus, R.J., van Westrenen, W., Woodhead, J.D., Jenner, F.E., Nebel-Jacobsen, Y. J., Wille, M., Eggins, S.M., 2013. Coupled Hf-Nd-Pb isotope co-variations of HIMU oceanic island basalts from Mangaia, Cook-Austral islands, suggest an Archean source component in the mantle transition zone. Geochimica et Cosmochimica Acta 112, 87–101.

Niu, Y.L., 2004. Bulk-rock major and trace element compositions of abyssal peridotites: Implications for mantle melting, melt extraction and post-melting processes beneath mid-ocean ridges. Journal of Petrology 45, 2423–2458.

Niu, Y.L., O'Hara, M.J., 2003. Origin of ocean island basalts: A new perspective from petrology, geochemistry, and mineral physics considerations. Journal of Geophysical Research-Solid Earth 108.

Nowell, G.M., Pearson, D.G., Bell, D.R., Carlson, R.W., Smith, C.B., Kempton, P.D., Noble, S.R., 2004. Hf isotope systematics of kimberlites and their megacrysts: New constraints on their source regions. Journal of Petrology 45, 1583–1612.

Parsons, B., 1982. Causes and consequences of the relation between area and age of the ocean-floor. Journal of Geophysical Research - Solid Earth 87, 289–302.

Paulick, H., Bach, W., Godard, M., De Hoog, J.C.M., Suhr, G., Harvey, J., 2006. Geochemistry of abyssal peridotites (Mid-Atlantic Ridge, 15 degrees 20 ' N, ODP Leg 209): Implications for fluid/rock interaction in slow spreading environments. Chemical Geology 234, 179–210.

Pilet, S., Baker, M.B., Stolper, E.M., 2008. Metasomatized lithosphere and the origin of alkaline lavas. Science 320, 916–919.

Ranero, C.R., Morgan, J.P., McIntosh, K., Reichert, C., 2003. Bending-related faulting and mantle serpentinization at the Middle America trench. Nature 425, 367–373.

Ranero, C.R., Sallares, V., 2004. Geophysical evidence for hydration of the crust and mantle of the Nazca plate during bending at the north Chile trench. Geology 32, 549–552.

Reisberg, L., Rouxel, O., Ludden, J., Staudigel, H., Zimmermann, C., 2008. Re-Os results from ODP Site 801: Evidence for extensive Re uptake during alteration of oceanic crust. Chemical Geology 248, 256–271.
Robertson, A.H.F., 2007. Geochemical evidence for the sedimentary and diagenetic development of the Mesozoic–early Cenozoic Newfoundland rifted margin, northwest Atlantic (Ocean Drilling Program Leg 210, Site 1276). In: Tucholke, B.E., Sibuet, J.-C., Klaus, A. (Eds.), Proc. ODP, Sci. Result 210, pp. 1–63 College Station TX.
Rowley, D.B., 2002. Rate of plate creation and destruction: 180 Ma to present. Geological Society of America Bulletin 114, 927–933.
Rudnick, R.L., Barth, M., Horn, I., McDonough, W.F., 2000. Rutile-bearing refractory eclogites: missing link between continents and depleted mantle. Science 287, 278–281.
Ryan, J.G., Chauvel, C., 2014. The subduction-zone filter and the impact of recycled materials on the evolution of the mantle. In: Turekian, K.K., Holland, H.D. (Eds.), Treatise on Geochemistry, 2nd Edition Vol. 3, pp. 479–508.
Salters, V.J.M., White, W.M., 1998. Hf isotope constraints on mantle evolution. Chemical Geology 145, 447–460.
Scambelluri, M., Fiebig, J., Malaspina, N., Muntener, O., Pettke, T., 2004. Serpentinite subduction: Implications for fluid processes and trace-element recycling. International Geology Review 46, 595–613.
Scambelluri, M., Pettke, T., van Roermund, H.L.M., 2008. Majoritic garnets monitor deep subduction fluid flow and mantle dynamics. Geology 36, 59–62.
Schmidt, W.W., Poli, S., 2014. Devolatilization during subduction. In: Turekian, K.K., Holland, H.D. (Eds.), Treatise on Geochemistry, 2nd Edition Vol. 4, pp. 669–701.
Schmidt, M.W., Vielzeuf, D., Auzanneau, E., 2004. Melting and dissolution of subducting crust at high pressures: the key role of white mica. Earth and Planetary Science Letters 228, 65–84.
Scott, J.M., Brenna, M., Crase, J.A., Waight, T.E., van der Meer, Q.H.A., Cooper, A.F., Palin, J. M., Le Roux, P., Munker, C., 2016. Peridotitic Lithosphere Metasomatized by Volatile-bearing Melts, and its Association with Intraplate Alkaline HIMU-like Magmatism. Journal of Petrology 57, 2053–2078.
Shields, G., Veizer, J., 2002. Precambrian marine carbonate isotope database: Version 1.1. Geochemistry Geophysics Geosystems 3, 12.
Singer, D. M., Maher, K., Brown, G. E. Jr., 2009. Uranyl-chlorite sorption/desorption: Evaluation of different U(VI) sequestration processes. Geochimica et Cosmochimica Acta 73, 5989–6007.
Spandler, C., Pirard, C., 2013. Element recycling from subducting slabs to arc crust: A review. Lithos 170, 208–223.
Spandler, C., Hermann, J., Arculus, R., Mavrogenes, J., 2003. Redistribution of trace elements during prograde metamorphism from lawsonite blueschist to eclogite facies; implications for deep subduction-zone processes. Contributions to Mineralogy and Petrology 146, 205–222.
Spandler, C., Mavrogenes, J., Hermann, J., 2007. Experimental constraints on element mobility from subducted sediments using high-P synthetic fluid/melt inclusions. Chemical Geology 239, 228–249.
Stacey, J.S., Kramers, J.D., 1975. Approximation of terrestrial lead isotope evolution by a two-stage model. Earth and Planetary Science Letters 26, 207–221.
Staudigel, H., 2014. Chemical Fluxes from Hydrothermal Alteration of the Oceanic Crust. In: Turekian, K.K., Holland, H.D. (Eds.), Treatise on Geochemistry, 2nd Edition Vol. 4, pp. 583–606.
Staudigel, H., Davies, G.R., Hart, S.R., Marchant, K.M., Smith, B.M., 1995. Large-scale isotopic Sr, Nd and O isotopic anatomy of altered oceanic-crust - DSDP/ODP Sites-417/418. Earth and Planetary Science Letters 130, 169–185.
Stern, R.A., Syme, E.C., Lucas, S.B., 1995. Geochemistry of 1.9 Ga MORB- and OIB-like basalts from the Amsik collage, Flin-Flon Belt, Canada: Evidence for an intra-oceanic origin. Geochimica et Cosmochimica Acta 59, 3131–3154.
Stracke, A., 2012. Earth's heterogeneous mantle: A product of convection-driven interaction between crust and mantle. Chemical Geology 330, 274–299.
Stracke, A., Bizimis, M., Salters, V.J.M., 2003. Recycling oceanic crust: Quantitative constraints. Geochemistry Geophysics Geosystems 4.
Sumner, D.Y., Grotzinger, J.P., 1996. Were kinetics of Archean calcium carbonate precipitation related to oxygen concentration? Geology 24, 119–122.
Syracuse, E.M., van Keken, P.E., Abers, G.A., 2010. The global range of subduction zone thermal models. Physics of the Earth and Planetary Interiors 183, 73–90.
Tackley, P.J., 2000. Mantle convection and plate tectonics: Toward an integrated physical and chemical theory. Science 288, 2002–2007.
Tsuru, A., Walker, R.J., Kontinen, A., Peltonen, P., Hanski, E., 2000. Re-Os isotopic systematics of the 1.95 Ga Jormua Ophiolite Complex, northeastern Finland. Chemical Geology 164, 123–141.
Ulmer, P., Trommsdorff, V., 1995. Serpentine stability to mantle depths and subduction-related magmatism. Science 268, 858–861.
van Keken, P.E., Hauri, E.H., Ballentine, C.J., 2002. Mantle mixing: The generation, preservation, and destruction of chemical heterogeneity. Annual Review of Earth and Planetary Sciences 30, 493–525.
Von Blanckenburg, F., O'Nions, R., Hein, J., 1996. Distribution and sources of pre-anthropogenic lead isotopes in deep ocean water from Fe Mn crusts. Geochimica et Cosmochimica Acta 60, 4957–4963.
Weaver, B.L., 1991. The origin of ocean island basalt end-member compositions - trace-element and isotopic constraints. Earth and Planetary Science Letters 104, 381–397.
Weiss, Y., Class, C., Goldstein, S.L., Hanyu, T., 2016. Key new pieces of the HIMU puzzle from olivines and diamond inclusions. Nature 537, 666–670.
White, W.M., 2015. Probing the earth's deep interior through geochemistry. Geochemical Perspectives 4, 95–251.
Willbold, M., Stracke, A., 2006. Trace element composition of mantle end-members: Implications for recycling of oceanic and upper and lower continental crust. Geochemistry Geophysics Geosystems 7, 30.
Zindler, A., Hart, S., 1986. Chemical geodynamics. Annual Review of Earth and Planetary Sciences 14, 493–571.